Cleavage of 3′,5′-Pyrophosphate-Linked Dinucleotides by Ribonuclease A and Angiogenin[†,‡]

Anwar M. Jardine,[§] Demetres D. Leonidas,[||,⊥] Jeremy L. Jenkins,[§] Chiwook Park,[#,▽] Ronald T. Raines,[#,○] K. Ravi Acharya,[||] and Robert Shapiro*[,§,@]

Center for Biochemical and Biophysical Sciences and Medicine and Department of Pathology, Harvard Medical School, Boston, Massachusetts 02115, Department of Biology and Biochemistry, University of Bath, Claverton Down, Bath BA2 7AY, U.K., and Department of Biochemistry and Department of Chemistry, University of Wisconsin, Madison, Wisconsin 53706

Received May 1, 2001; Revised Manuscript Received June 12, 2001

ABSTRACT: Recently, 3′,5′-pyrophosphate-linked 2′-deoxyribodinucleotides were shown to be >100-fold more effective inhibitors of RNase A superfamily enzymes than were the corresponding monophosphate-linked (i.e., standard) dinucleotides. Here, we have investigated two ribo analogues of these compounds, cytidine 3′-pyrophosphate (P′→5′) adenosine (CppA) and uridine 3′-pyrophosphate (P′→5′) adenosine (UppA), as potential substrates for RNase A and angiogenin. CppA and UppA are cleaved efficiently by RNase A, yielding as products 5′-AMP and cytidine or uridine cyclic 2′,3′-phosphate. The k_{cat}/K_m values are only 4-fold smaller than for the standard dinucleotides CpA and UpA, and the K_m values (10−16 μM) are lower than those reported for any earlier small substrates (e.g., 500−700 μM for CpA and UpA). The k_{cat}/K_m value for CppA with angiogenin is also only severalfold smaller than for CpA, but the effect of lengthening the internucleotide linkage on K_m is more modest. Ribonucleotide 3′,5′-pyrophosphate linkages were proposed previously to exist in nature as chemically labile intermediates in the pathway for the generation of cyclic 2′,3′-phosphate termini in various RNAs. We demonstrate that in fact they are relatively stable ($t_{1/2}$ > 15 days for uncatalyzed degradation of UppA at pH 6 and 25 °C) and that cleavage in vivo is most likely enzymatic. Replacements of the RNase A catalytic residues His12 and His119 by alanine reduce activity toward UppA by $\sim 10^5$-and $10^{3.3}$-fold, respectively. Thus, both residues play important roles. His12 probably acts as a base catalyst in cleavage of UppA (as with RNA). However, the major function of His119 in RNA cleavage, protonation of the 5′-O leaving group, is not required for UppA cleavage because the pK_a of the leaving group is much lower than that for RNA substrates. A crystal structure of the complex of RNase A with 2′-deoxyuridine 3′-pyrophosphate (P′→5′) adenosine (dUppA), determined at 1.7 Å resolution, together with models of the UppA complex based on this structure suggest that His119 contributes to UppA cleavage through a hydrogen bond with a nonbridging oxygen atom in the pyrophosphate and through $\pi-\pi$ stacking with the six-membered ring of adenine.

Bovine pancreatic ribonuclease A (RNase A; EC 3.1.27.5)[1] and its homologues comprise a functionally diverse superfamily of enzymes that catalyze the cleavage of P−$O^{5'}$ bonds in RNA on the 3′ side of pyrimidines to form cyclic 2′,3′-phosphates (for reviews, see refs *1*−*4*). Pancreatic RNase exhibits the highest catalytic efficiency of any known superfamily member and has been considered to play a largely digestive role. Angiogenin (Ang), which has the

[†] This work was supported by the National Institutes of Health (Grants HL52096 to R.S. and GM44783 to R.T.R.), the Medical Research Council (Republic of South Africa; Overseas Scholarship to A.M.J.), and the Medical Research Council (U.K.) (Programme Grant 9540039 to K.R.A.).

[‡] The atomic coordinates for the complex of ribonuclease A with dUppA have been deposited with the Protein Data Bank (accession number 1JN4).

* To whom correspondence should be addressed. Telephone: 617-432-4010; fax: 617-566-3137; e-mail: Robert_Shapiro@hms.harvard.edu.

[§] Center for Biochemical and Biophysical Sciences and Medicine, Harvard Medical School.

[||] Department of Biology and Biochemistry, University of Bath.

[⊥] Present address: Institute of Biological Research and Biotechnology, The National Hellenic Research Foundation, 48 Vas. Constantinou Avenue, Athens 11635, Greece.

[#] Department of Biochemistry, University of Wisconsin.

[▽] Present address: Department of Molecular and Cell Biology, University of California, Berkeley, 229 Stanley Hall, Berkeley, CA 94720.

[○] Department of Chemistry, University of Wisconsin.

[@] Department of Pathology, Harvard Medical School.

[1] Abbreviations: RNase A, ribonuclease A; Ang, angiogenin; pdUppA-3′-p, 5′-phospho-2′-deoxyuridine 3′-pyrophosphate (P′→5′) adenosine 3′-phosphate; CppA, cytidine 3′-pyrophosphate (P′→5′) adenosine; UppA, uridine 3′-pyrophosphate (P′→5′) adenosine; mpA, adenosine 5′-monophosphomorpholidate; U-3′-p, uridine 3′-phosphate; dU-3′-p, 2′-deoxyuridine 3′-phosphate; C-3′-p, cytidine 3′-phosphate; A-5′-ppA, adenosine 5′-pyrophosphate (P→5′) adenosine; Ches, 2-(*N*-cyclohexylamino)ethanesulfonic acid; TEAB, triethylammonium bicarbonate; BSA, bovine serum albumin; A-5′-p, adenosine 5′-phosphate; dUppA, 2′-deoxyuridine 3′-pyrophosphate (P′→5′) adenosine; FABMS, fast atom bombardment mass spectrometry; UpA, uridylyl(3′→5′) adenosine; CpA, cytidylyl(3′→5′) adenosine; C>p, cytidine cyclic 2′,3′-phosphate; U>p, uridine cyclic 2′,3′-phosphate; PEG, poly(ethylene glycol); PDB, Protein Data Bank (http://www.rcsb.org/pdb/); TppdA, thymidine 3′-pyrophosphate (P′→5′) 2′-deoxyadenosine; dUppA-3′-p, 2′-deoxyuridine 3′-pyrophosphate (P′→5′) adenosine 3′-phosphate; rms, root mean square; UpcA, UpA with the 5′-oxygen of the adenosine ribose replaced by a methylene group; ppA, adenosine 5′-diphosphate; ppA-2′-p, 5′-diphosphoadenosine 2′-phosphate; $UpOC_6H_4$-*p*-NO_2, uridine 3′-(*p*-nitrophenyl) phosphate.

10.1021/bi010888j CCC: $20.00
Published on Web 08/02/2001

lowest activity toward standard RNase substrates (*5*), is an inducer of new blood vessel formation in vivo (*6*) and has been shown to be critical for the establishment and metastatic spread of tumors in mice (*7*, *8*). RNase 2 (also known as eosinophil-derived neurotoxin) is nearly as potent as the pancreatic enzyme (*9*), whereas RNase 3 (eosinophil cationic protein) is relatively weak (*10*); both have host defense-related activities (*11*−*14*) but are also neurotoxic and may be involved in some eosinophil-associated diseases (*15*−*17*). Yet, other homologues have been shown (*18*) or are suspected (*19*) to have unusual biological activities, and it is possible that none of the RNases, including the pancreatic enzyme, have exclusively digestive functions as originally envisioned.

The vast majority of the physiological actions of the RNases appear to be strictly dependent on ribonucleolytic activity (*11*, *12*, *20*−*22*). Recognition of this relationship has spurred efforts to develop tight-binding small-molecule inhibitors that could be used to elucidate the in vivo roles of the various RNases and to treat diseases associated with these proteins. One promising group of inhibitors identified consists of novel dinucleotides with the structure (*x*)dNpp-(d)A*y*, where dN is a 2′-deoxyribopyrimidine nucleoside, (d)A is ribo- or 2′-deoxyriboadenosine, pp is a pyrophosphate linking the 3′-oxygen of dN with the 5′-oxygen of (d)A, *x* is an optional 5′-phosphate, and *y* is a 3′- or 2′-phosphate (*23*). The most effective compounds bind to RNase A, RNase 2, and RNase 4 with K_i values in the mid-to-upper nanomolar range and to Ang with midmicromolar K_i's (*24*, *25*). The pyrophosphate linkage is a key factor contributing to high affinity and increases potency toward RNase A by 2 orders of magnitude as compared to the usual monophosphate internucleotide linkage.

A crystal structure of the complex of RNase A with the tightest of these ligands, pdUppA-3′-p [5′-phospho-2′-deoxyuridine 3′-pyrophosphate (P′→5′) adenosine 3′-phosphate; K_i value 27 nM] has been determined (*26*). In this structure, adenosine adopts a syn conformation with a glycosyl torsion angle that differs by nearly 180° from those observed in previous RNase A complexes, which are all in the anti range. This conformation allows adenine and uracil to occupy the same nucleobase-binding subsites as their counterparts in normal dinucleotides, despite the extended internucleotide linker. The rotated adenine ring forms a set of interactions with the protein that seem to be even more favorable than those made by the base in its normal anti orientation. The interactions of the uridine 3′-phosphate portion of pdUppA-3′-p are essentially the same as those of corresponding parts of noncleavable substrate analogues in earlier structures (*3*, *27*, *28*), which are assumed to resemble those of RNA substrates themselves; this suggests that 3′,5′-pyrophosphate-linked dinucleotides, in which the pyrimidine nucleoside sugar is ribose rather than 2′-deoxyribose, would be substrates instead of inhibitors. RNase A is known to have broad tolerance with respect to leaving groups. In addition to the normal nucleoside 5′-O, a wide variety of alkyl and aryl oxygens are acceptable (*29*−*31*). Moreover, the preference of RNase A for the pyrophosphate vs monophosphate group as internucleotide linkage in inhibitors would be expected to translate into a lower K_m with substrates.

Here, we report that cytidine 3′-pyrophosphate (P′→5′) adenosine (CppA) and uridine 3′-pyrophosphate (P′→5′) adenosine (UppA) are indeed excellent substrates for RNase A, with k_{cat}/K_m values only 4-fold smaller than for CpA and UpA and K_m values lower than those reported for any previous small substrates. We demonstrate that this class of compound, which was previously thought to be chemically labile (*32*, *33*), is in fact relatively long-lived under conditions typical for RNase assays. We also present the results of mutational and crystallographic studies on the interactions of these dinucleotides with RNase A and the implications of our findings for the catalytic mechanism. Finally, we describe the kinetic behavior of the pyrophosphate-linked dinucleotides with a second RNase superfamily enzyme, Ang.

EXPERIMENTAL PROCEDURES

Materials and General Procedures. CpA; UpA; adenosine 5′-monophosphomorpholidate (mpA) 4-morpholine-*N*,*N*-dicyclohexylcarboxamidinium salt; the monosodium salts of uridine 3′-phosphate (U-3′-p), 2′-deoxyuridine 3′-phosphate (dU-3′-p), and cytosine 3′-phosphate (C-3′-p); adenosine 5′-pyrophosphate (P→5′) adenosine (A-5′-ppA); 2-(*N*-cyclohexylamino)ethanesulfonic acid (Ches); and nucleotide standards for chromatography were purchased from Sigma. Anhydrous pyridine was obtained from Aldrich and used without further purification. 1*H*-Tetrazole was from Amersham-Pharmacia. RNase A, Ang (Pyr-1 form), and RNase A variants H12A and H119A were obtained and quantified as described previously (*34*−*36*). Alkaline phosphatase (*Escherichia coli*, type III) from Sigma was dissolved in 10 mM Tris, pH 8.0, to a concentration of 15 μM. Stock solutions of triethylammonium bicarbonate (TEAB) were prepared by mixing triethylamine (Pierce, sequanal grade) with water and then titrating the pH with CO_2 gas (from dry ice) with rapid stirring. Mes was purchased from Calbiochem. The following precautions were taken to minimize the amount of adventitious RNase in stocks of substrate and inhibitor and in enzymatic assays: (1) Water and buffer solutions were passed through a Sep-Pak C18 cartridge (Waters) and collected in fresh plastic tubes or in glass bottles that had been treated with base [0.1 N NaOH for >2 h followed by extensive rinsing with water directly from a Milli-Q system (Millipore)]. (2) The HPLC system used for purification of substrates and inhibitor was cleaned by injecting 2 mL of 2 N sodium hydroxide and then pumping water through the system for 30 min at a flow rate of 0.2 mL/min. (3) The protein carrier used to prevent adsorption of RNase A to assay cuvettes was RNase-free bovine serum albumin (BSA; Worthington). All operations were conducted at ambient temperature unless specified otherwise. Mass spectrometry was performed by the Department of Chemistry and Chemical Biology at Harvard University.

Synthesis and Purification of 3′,5′-Pyrophosphate-Linked Dinucleotides. Pyrophosphate-linked dinucleotides NppA and dNppA were prepared by a modification of methods used previously (*23*, *37*). Nucleotides (0.18 mmol for U-3′-p and C-3′-p, 0.06 mmol for dU-3′-p) were dissolved in water and then treated with Dowex 50W-X8 cation-exchange resin (tributylammonium form, 4 mL) for 10 min. The resin was filtered and washed with water, and the filtrate was lyophilized to give the corresponding tributylammonium nucleotide salts. This material was combined with mpA (0.07 mmol), and the mixture was coevaporated with anhydrous pyridine (typically 1 mL, 3×) and dried over phosphorus pentoxide

for 2 days under vacuum. Anhydrous pyridine (1.5−2.0 mL) was then added, and the solution was stirred for 5 days in a dry nitrogen atmosphere; for the reaction with U-3′-p, 1*H*-tetrazole (0.07 mmol) was also included. The mixture was then diluted with an equal volume of water, evaporated under reduced pressure until most of the pyridine had been removed, diluted with water, lyophilized, and redissolved in water. An aliquot of each mixture was analyzed by anion-exchange chromatography on a Mono Q column (HR5/5; Amersham Pharmacia Biotech); a 30-min linear gradient from 40 to 190 mM TEAB, pH 7.6, was applied at a flow rate of 1 mL/min, and the absorbance of the effluent at 254 nm was recorded. At least four major peaks were observed in all instances. The peak representing the desired NppA or dNppA product was identified by comparing this chromatogram with those obtained for the starting materials (mpA, N-3′-p, and 1*H*-tetrazole), adenosine 5′-phosphate (A-5′-p; formed by hydrolysis of mpA), and A-5′-ppA (another byproduct). Assignments (peaks with retention times of 19.3, 17.03, and 20.0 min as UppA, CppA, and dUppA, respectively) were confirmed by the effects of incubating a second sample aliquot with pyrophosphatase (*24*): in each case, the size of the putative dinucleotide peak was reduced greatly, and the peaks corresponding to A-5′-p and N-3′-p became much larger. Dinucleotide products were then purified in 0.5−2-mg batches by chromatography in the same system used for analysis. The CppA mixture was incubated with alkaline phosphatase (2.5 μM for 30 min at 25 °C in 15 mM Mes/NaOH and 15 mM NaCl, pH 6.0) prior to chromatography to eliminate nucleoside monophosphate contaminants, which did not resolve as fully as for the UppA and dUppA mixtures. Material eluting at the expected time for each dinucleotide was diluted with an equal volume of water, lyophilized, and reconstituted in water. The purity of the final product, as assessed by Mono Q chromatography with a 25-min linear gradient of 30−200 mM NaCl in 10 mM Tris, pH 8.0, at 1.2 mL/min was >90% in all cases. FABMS results were in excellent agreement with the proposed structures: $[M - H]^- = 652.0803$ for UppA (calculated for $C_{19}H_{25}N_7O_{15}P_2 = 653.0884$); $[M - H]^- = 651.0962$ for CppA (calculated for $C_{19}H_{26}N_8O_{14}P_2 = 652.1044$); and $[M - H]^- = 636.0852$ for dUppA (calculated for $C_{19}H_{25}N_7O_{14}P_2 = 637.0935$).

Enzymatic Assays. Assays were performed in 0.1 M Mes/NaOH, pH 6.0, containing 0.1 M NaCl and 10 μg/mL BSA at 25 °C unless specified otherwise. Concentrations of substrate and inhibitor solutions were determined spectrophotometrically; the ϵ_{260} values used (25 000 M^{-1} cm^{-1} for UpA, UppA, and dUppA; 22 600 M^{-1} cm^{-1} for CpA and CppA) were calculated from those for mononucleotides listed by Beaven et al. (*38*). Values of k_{cat}/K_m for cleavage of CpA and UpA by RNase A and its H12A and H119A variants were determined by a modification of the spectrophotometric assay of Witzel and Barnard (*29*). The absorbance decrease at 286 (CpA) or 280 nm (UpA) produced by conversion of substrate (50 μM) to products [adenosine and either cytidine cyclic 2′,3′-phosphate (C>p) or uridine cyclic 2′,3′-phosphate (U>p)] was monitored continuously (data points collected every 1−2 s) with a Cary 1E instrument during the complete reaction. The data were then fitted to a first-order process with SigmaPlot 4.0 (SPSS), and the rate constant was divided by the enzyme concentration (1−3 nM for RNase A, 31.6 μM for H12A, and 33.0 μM for H119A) to give k_{cat}/K_m. The reactions were expected to be first-order because (i) the substrate concentration is well below K_m (*39*, *40*), (ii) the hydrolysis of cyclic nucleotide products during the assay (which would increase the absorbance) is at least several hundred-fold slower than dinucleotide cleavage (*29*), and (iii) the products bind very weakly (*3*). Indeed, all curve fits yielded r^2 values >0.999. The K_i value for inhibition of RNase A by dUppA was determined by measuring k_{cat}/K_m values for UpA cleavage at five inhibitor concentrations ranging from 5 to 60 μM. The data were fitted to the equation $(k_{cat}/K_m)_i = (k_{cat}/K_m)_0/(1 + [I]/K_i)$ with SigmaPlot, where $(k_{cat}/K_m)_i$ and $(k_{cat}/K_m)_0$ are values measured in the presence and absence of inhibitor I, respectively.

Cleavage of CppA and UppA by RNase A was monitored spectrophotometrically as with CpA and UpA. (The assay for standard dinucleotides is based on the shift in UV absorbance spectrum associated with conversion of the N-3′-p portion of the substrate to the corresponding N>p; this same conversion occurs with the pyrophosphate-linked dinucleotides.) Values for k_{cat} and K_m were determined from progress curves for the entire reaction, fitting the data to the equation for the integrated Michaelis−Menten equation

$$([S]_0 - [S])/t = (k_{cat}[E]) - (K_m/t)\ln([S]_0/[S])$$

with SigmaPlot, where $[S]_0$ and [S] are substrate concentrations at the beginning of the recorded reaction (<1 min after addition of enzyme) and at time *t*, respectively. Data for the first 10% and last 15% of the reaction were not included because they are statistically problematic. All values of r^2 for the fits obtained were >0.996. The initial substrate concentrations used were 37−51 μM for CppA and 30−40 μM for UppA; concentrations during the reaction were calculated by using $\Delta\epsilon_{286} = 1453$ M^{-1} cm^{-1} (CppA) and $\Delta\epsilon_{280} = 1700$ M^{-1} cm^{-1} (UppA), which were based on the absorbance change for complete conversion of each substrate to products. The enzyme concentrations were 2−4.5 nM. Alkaline phosphatase (0.5 μM) was included in the reaction mixtures to convert inhibitory nucleotide products to their respective nucleosides (see Results). The effectiveness of the phosphatase treatment for eliminating A-5′-p was assessed by Mono Q chromatography with the NaCl gradient described above. Kinetic parameters for cleavage of UppA by H119A-RNase A were determined as for wild-type RNase A, except that the substrate and enzyme concentrations were 102−127 and 5.9 μM, respectively. Cleavage of UppA by H12A-RNase A was too slow to allow accurate monitoring of the complete reaction, and initial velocity (v_0) (first 10% of the reaction) was measured instead with 31.6 μM enzyme and 36 μM substrate.

Values of k_{cat}/K_m for cleavage of CpA, UpA, and CppA by Ang were measured by a modification of previous methods (*25*, *39*). Incubations were performed with 10−17 μM enzyme and ~100 μM substrate in 0.2 M Mes/NaOH, pH 5.9, or in the same assay buffer used for RNase A but without BSA. After various times covering 1−2 half-lives of the reaction, aliquots were analyzed by Mono Q chromatography with the NaCl gradient described above (CppA), with a linear 10-min gradient from 0 to 0.1 M NaCl in 10 mM Tris, pH 8, at 1 mL/min (UpA) or by isocratic elution with 10 mM Tris, pH 8, containing 30 mM NaCl (CpA).

Values for k_{cat}/K_m were then calculated from the extents of substrate cleavage, as indicated from the amount of remaining substrate (for CppA), or from both substrate and products (for CpA and UpA); values reported are averages of 2−4 determinations. The substrate concentration is well below K_m for CpA (*41*) and CppA (shown below) and is assumed to be $\ll K_m$ for the less efficient substrate UpA as well. Incubation times were 90−110 min for CpA, 2−18 h for UpA, and 100 min−23 h for CppA. [A control experiment showed that Ang retains full enzymatic activity for at least 24 h under these conditions (results not shown).] The rate constant for CppA cleavage in the absence of Ang was <5% of the Ang-catalyzed rate. Similar k_{cat}/K_m values were obtained for two preparations of Ang; in both cases, assays with UpA as the substrate revealed activities ~20-fold lower than with CpA, demonstrating that these preparations do not contain significant amounts of contaminating RNase A (which exhibits only a ~2-fold preference for CpA vs UpA; *42*). Initial velocities for cleavage of CppA (94 μM and 2.6 mM) by Ang (10 and 50 μM, respectively) in 0.2 M Mes/NaOH, pH 5.9 (the standard assay conditions for Ang; *41*), were measured by using Mono Q chromatography to follow the decrease in substrate concentration during the first 10−15% of the reaction. The aliquots analyzed were 20 μL (out of 100 μL) for the lower CppA concentration and 1 μL (out of 25 μL; diluted to 30 μL in water) for the higher concentration.

Nonenzymatic Cleavage of UpA and UppA. Dinucleotides (100−130 μM) were incubated at 25 °C in either 0.1 M Mes/NaOH, pH 6.0, containing 0.1 M NaCl or 30 mM Ches/NaOH, pH 10. At various times, aliquots of 10−20 μL (out of 100−200 μL) were analyzed by Mono Q chromatography with the Tris/NaCl systems described for these nucleotides above. The pH 10 samples were diluted 5-fold with 75 mM Mes/NaOH, pH 5.9, prior to injection onto the column. The percentage of UppA cleaved was calculated from the peak areas at 254 nm for U>p and UppA; the area per nanomole for UppA is 2.14× that for U>p (based on the measured $\Delta\epsilon_{254}$ for full conversion of UpA to U>p and A and spectral data for U and A; *38*). UppA reactions were monitored for 1−2 half-lives (12 days at pH 6, 90 min at pH 10; 3−5 data points). For UpA, which was examined only at pH 10, the extent of cleavage was calculated from the peak areas for UpA and U-2′(3′)-p; the area per nanomole for UpA is 2.54× that for the two product isomers, which coelute. The reaction was monitored for 15 days (3 data points).

Crystallography. RNase A crystals were grown using the vapor-diffusion technique as described in ref *43*; they belong to the space group C2, with two molecules per asymmetric unit. Crystals of the RNase·dUppA complex were obtained by soaking the RNase A crystals in 50 mM dUppA, 20 mM sodium citrate, pH 5.5, and 25% PEG 4000 for 24 h.

Diffraction data were collected on a 30 cm diameter MAR-Research image plate system mounted on an Enraf Nonius X-ray generator at 100 K (the reservoir buffer with 30% PEG 400 was used as cryoprotectant). All data were processed using the XDS package (*44*). The data processing statistics are given in Table 1.

Phases were obtained using the structure of free RNase A (*43*) as a starting model. Alternating cycles of manual building, conventional positional refinement, simulated annealing, and finally solvent corrections, as implemented in X-Plor 3.851 (*45*), improved the model. The inhibitor molecule was included during the final stages of the refinement using the atomic coordinates of pdUppA-3′-p from the crystal structure of the RNase A·pdUppA-3′-p complex (PDB code 1qhc; *26*). The inhibitor was found only in molecule 1 of the noncrystallographic dimer, although pdUppA-3′-p binds to both RNase A molecules; this difference probably reflects the 400-fold tighter binding of the larger dinucleotide. Details of the refinement are provided in Table 1.

Table 1: Crystallographic Statistics

Data Collection Statistics	
space group	C2 (two molecules per asymmetric unit)
a (Å)	99.8
b (Å)	32.3
c (Å)	72.1
β (°)	90.1
resolution (Å)	30−1.8
reflections measured	41852
unique reflections	18095
R_{sym} (%)[a]	8.6 (26.2)
completeness (outermost shell 1.91−1.8 Å) (%)	84.5 (80.8)
temperature (K)	100
Refinement Statistics	
R_{cryst} (%)[b]	22.5
R_{free} (%)[c]	29.5
no. of protein atoms	1902
no. of solvent molecules	265
rms deviation from ideality in bond lengths (Å)	0.009
rms deviation from ideality in bond angles (°)	1.4
average B factor (Å^2)	
protein atoms (mol I/mol II)	25.4/24.0
solvent atoms	36.4
ligand atoms (mol I)	32.3

[a] $R_{sym} = \sum_h\sum_i|I(h) - I_i(h)|/\sum_h\sum_i I_i(h)$, where $I_i(h)$ and $I(h)$ are the *i*th and the mean measurements of the intensity of reflection *h*. [b] $R_{cryst} = \sum_h|F_o - F_c|/\sum_h F_o$, where F_o and F_c are the observed and calculated structure factor amplitudes of reflection *h*, respectively. [c] R_{free} is equal to R_{cryst} for a randomly selected 5% subset of reflections not used in the refinement (*72*).

Molecular Modeling. Modeling was performed with Insight II (Molecular Simulations) implemented on a Silicon Graphics IndigoII Maximum Impact work station. The Insight II module FDiscover (Molecular Simulations) was used for energy minimization. Atomic potentials and partial charges were assigned using the Amber force field. The steepest descent algorithm was employed for initial minimization, followed by conjugate gradient and BFGS algorithms, for a total of 500 iterations; application of this program to the crystal structure of the dUppA·RNase A complex produced no significant changes. Docking of a UppA model to RNase A was done with the AutoDock 3.0 (*46*) Lamarckian Genetic Algorithm using default-generated parameters, except that 1.5×10^6 energy evaluations were used for 15 docking runs. The coordinates for dUppA from the dUppA·RNase A complex structure were used as the grid center in the grid parameter file and as the initial position ($tran_0$) in the docking parameter file.

RESULTS

Cleavage of Dinucleoside Pyrophosphates by RNase A. The most effective normal dinucleotide substrates of RNase

Table 2: Kinetic Parameters for Cleavage of UppA, CppA, UpA, and CpA by RNase A[a]

substrate	K_m (μM)	k_{cat} (s^{-1})	k_{cat}/K_m (M^{-1} s^{-1})
UppA	9.9 ± 1.3	7.7 ± 0.6	$(7.8 \pm 0.5) \times 10^5$
CppA	16.4 ± 1.3	26.0 ± 2.0	$(1.59 \pm 0.04) \times 10^6$
UpA[b]	[700]	[2690]	$(3.0 \pm 0.1) \times 10^6$ [3.8×10^6]
CpA[c]	[500]	[2300]	$(6.4 \pm 0.7) \times 10^6$ [4.6×10^6]

[a] Assay conditions: 0.1 M Mes/NaOH and 0.1 M NaCl, pH 6.0, at 25 °C. Kinetic parameters not in brackets were determined from progress curves as described in Experimental Procedures. Values listed are mean ±SD ($n = 3$). [b] Values shown in brackets are from Shapiro et al. (*39*); data were collected under conditions identical to those used here. [c] Values shown in brackets are from Shapiro and Vallee (*40*); the conditions were 33 mM Mes/NaOH and 33 mM NaCl, pH 6.0, at 25 °C.

A are CpA and UpA (*29*), which are cleaved with k_{cat}/K_m values of 6.4×10^6 and 3.0×10^6 M^{-1} s^{-1}, respectively (Table 2). The dinucleoside pyrophosphate analogues of these substrates, CppA and UppA, were synthesized by modifications of the procedures used previously for TppdA and dUppA-3′-p (*23*). Mono Q chromatographic analysis of aliquots of the two dinucleotides, following incubation with RNase A, revealed that both are substrates and that the cleavage products, as anticipated, are A-5′-p and C>p or U>p.

Measurements of v_0 for RNase A-catalyzed cleavage of 50 and 100 μM CppA and UppA in a spectrophotometric assay suggested that the K_m values are well below 50 μM. We therefore opted to determine the kinetic parameters for these reactions from progress curves (i.e., applying the integrated Michaelis−Menten equation) rather than from plots of v_0 vs substrate concentration, as are generally used with standard dinucleotides. With this method, a single assay performed at an initial substrate concentration greater than K_m yields values for both K_m and k_{cat}. For the approach to be valid, enzyme-catalyzed hydrolysis of the cyclic nucleotide product and product inhibition must be insignificant during the full course of the assay. The first requirement is clearly satisfied because the v_0 values measured are several 100-fold faster than for the C>p and U>p hydrolytic reactions; moreover, no increase in absorbance (which would be produced by hydrolysis) can be detected for at least several minutes after cleavage is completed. Inhibition by the cyclic nucleotide is also negligible because K_m for the substrate is at least hundred-fold lower than that for the product (*29*). However, inhibition by the other product (A-5′-p, whose K_i value is 80 μM; *47*) might interfere with the kinetic measurements. This problem was eliminated by including alkaline phosphatase in the reaction mixtures to convert A-5′-p into adenosine, which has a K_i value at least 20-fold higher (*48*). Analysis of aliquots of the assay mixtures at various times by Mono Q chromatography showed that the concentration of phosphatase used (0.5 μM) was sufficient to rapidly dephosphorylate any A-5′-p formed. This amount of phosphatase has no effect on k_{cat}/K_m for cleavage of UpA by RNase A (data not shown).

The progress curve data fit well to the integrated Michaelis−Menten equation (see, e.g., Figure 1), yielding K_m and k_{cat} values of 9.9 μM and 7.7 s^{-1}, respectively, for UppA and 16.4 μM and 26.0 s^{-1}, respectively, for CppA (Table 2). The K_m and k_{cat} values for UppA are 70- and 340-fold lower than those measured previously for UpA under the same conditions, and the resultant value for k_{cat}/K_m is 4-fold lower than that determined for UpA in the present set of experiments. The value of k_{cat}/K_m for CppA is also 4-fold lower than for CpA; thus, the C vs U selectivity is the same for both monophosphate- and pyrophosphate-linked dinucleotides.

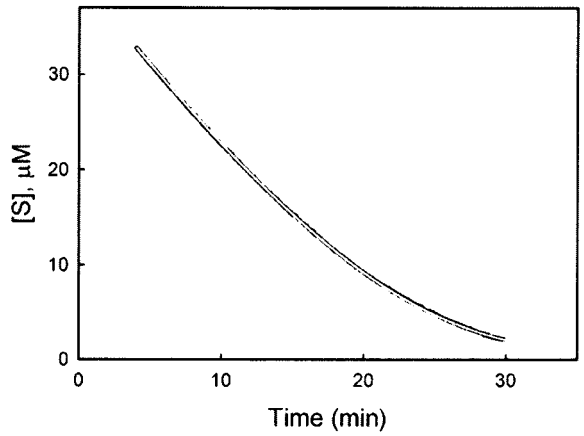

FIGURE 1: Cleavage of UppA (40 μM) by RNase A (4.5 nM) in 0.1 M Mes/NaOH and 0.1 M NaCl, pH 6.0, at 25 °C. The reaction was followed by monitoring the decrease in absorbance at 280 nm. The white line represents the best fit of the data to the integrated Michaelis−Menten equation (see Experimental Procedures).

Table 3: Chemical Stability of UppA and UpA[a]

dinucleotide	pH	k (s^{-1})	$t_{1/2}$
UppA[b,c]	6[d]	$<(5.3 \pm 1.3) \times 10^{-7}$	>15 d
UpA[c,e]	6	$<5 \times 10^{-9}$	>4 yr
UppA[b]	10[f]	$(2.4 \pm 0.4) \times 10^{-4}$	49 min
UpA[b]	10[f]	$(9.4 \pm 0.4) \times 10^{-8}$	85 d

[a] All reactions were at 25 °C. [b] Degradation was monitored by Mono Q chromatography as described in Experimental Procedures. [c] Rate constant listed is an upper limit (see text). [d] 0.1 M Mes/NaOH and 0.1 M NaCl. [e] Value listed is from Thompson et al. (*62*); the conditions were 50 mM Mes/HCl and 0.1 M NaCl. [f] 30 mM Ches-NaOH.

Chemical Stability of UppA. The uncatalyzed rate of UppA cleavage under the standard assay conditions was assessed by incubating the substrate without any added RNase A and measuring the extent of cleavage at various times by Mono Q chromatography. Loss of the dinucleotide occurred with a first-order rate constant of 5.3×10^{-7} s^{-1} ($t_{1/2} = 15$ days; Table 3). The only uridine product detected was U>p: that is, no significant amounts of U-3′-p or U-2′-p were formed. Therefore, as explained in the Discussion, it is unclear whether the degradation observed in fact reflects the uncatalyzed reaction or whether it is due to RNase contaminants, and the rate constant measured must be regarded only as an upper limit for the true value. Additional experiments on UppA and UpA were conducted at pH 10 (Table 3), where the uncatalyzed reaction is much more rapid and any RNases present would probably be less effective. The first-order rate constant for degradation of UppA to A-5′-p and U>p (the only uridine product) was 2.4×10^{-4} s^{-1}, corresponding to a half-life of 49 min. Cleavage of UpA proceeded at a 2500-fold slower rate than that of UppA; in this case, the major uridine products detected were U-3′-p and U-2′-p.

Activity of RNase A Variants H12A and H119A toward UppA. The roles of the catalytic residues His12 and His119 in catalyzing cleavage of UppA were examined by measuring the effects of replacing these residues individually by Ala.

Table 4: Cleavage of UppA and UpA by H12A and H119A RNase A Variants[a]

enzyme	substrate	K_m (μM)	k_{cat} (s^{-1})	k_{cat}/K_m (M^{-1} s^{-1})	$(k_{cat}/K_m)^{var}/(k_{cat}/K_m)^{wt}$
wild type	UppA	9.9 ± 1.3	7.7 ± 0.6	$(7.8 \pm 0.5) \times 10^5$	
H12A[b]	UppA			1.4−8	$1.7-10 \times 10^{-6}$
H119A	UppA	27.6 ± 6.4	0.0106 ± 0.0025	383 ± 13	4.9×10^{-4}
wild type[c]	UpA	[700]	[2690]	$(3.0 \pm 0.1) \times 10^6$	
H12A	UpA			26.4 ± 1.6	8.8×10^{-6}
H119A	UpA			27.0 ± 1.6	9.0×10^{-6}

[a] Conditions as listed in Table 2. [b] Cleavage of UppA by H12A was too slow to allow precise measurement of kinetic parameters (see Results). [c] Values in brackets are from Shapiro et al. (*39*); data were collected under conditions identical to those used here.

These substitutions were shown previously to have little effect on the 3D structure of RNase A but to decrease both its affinity for nucleotides and its k_{cat} and k_{cat}/K_m for cleaving standard substrates (*35*, *49*). For H119A, activity toward UppA was sufficiently high so that k_{cat} and K_m could be measured by the same method as with wild-type RNase A. The values obtained were 0.0106 s^{-1} and 27.6 μM (Table 4), respectively; the first value is 730-fold lower than that with the wild-type enzyme, whereas the latter represents a ~3-fold increase. The value for k_{cat}/K_m, 383 M^{-1} s^{-1}, is then 2000-fold smaller than that for the wild-type protein. The activity of H12A toward UppA was considerably weaker, and it was impractical to monitor the entire cleavage reaction, even when very high enzyme concentrations (up to 32 μM) were used. Moreover, the extremely slow initial rates measured were not accurate enough to allow the use of the standard approach (plots of v_0 vs [S]) for determination of the kinetic parameters: for example, v_0 measured with 36 μM UppA and 32 μM H12A was only $\sim 1.6 \times 10^{-9}$ M s^{-1}. However, these data can at least provide a basis for estimating a range of values for k_{cat}/K_m. Assuming that K_m for UppA is greater than or equal to that for wild-type RNase A, the calculated range for k_{cat}/K_m (taking into account depletion of free substrate by enzyme) is 1.4−8 M^{-1} s^{-1}, with the lower limit applying if K_m is well above the substrate concentration and the upper limit applying if K_m is not affected by the amino acid replacement. Thus, the loss of catalytic efficiency toward UppA for H12A is 50−270× greater than for H119A.

Crystal Structure of the Complex of RNase A with dUppA. The 3D structure of the complex of RNase A with the noncleavable UppA analogue dUppA was determined in order to facilitate interpretation of the kinetic and mutational data on cleavage of the dinucleoside pyrophosphates. [Although a structure of the complex of RNase A with pdUppA-3′-p was already available (*26*), we considered it possible that the interactions of the dUppA portion of pdUppA-3′-p might differ from those of dUppA itself in significant respects; in particular, the contacts of the 3′-phosphate in the pdUppA-3′-p are energetically strong and might have influenced those of A-5′-p.] dUppA was synthesized and purified as for UppA and was found to inhibit RNase A with a K_i value of 11.3 ± 0.2 μM, almost identical to the K_m for UppA. The dUppA·RNase A complex structure superimposes well with that of the pdUppA-3′-p complex: rms deviations are 0.325 Å for RNase α-carbons and 0.425 Å for dUppA with all corresponding atoms of pdUppA-3′-p. As in the earlier complex, uridine binds in an anti conformation, and its ribose adopts a C2′-endo pucker (*50*). Adenosine again binds in a syn conformation, but its furanose conformation (C4′-exo) differs from that in pdUppA-3′-p (C2′-endo).

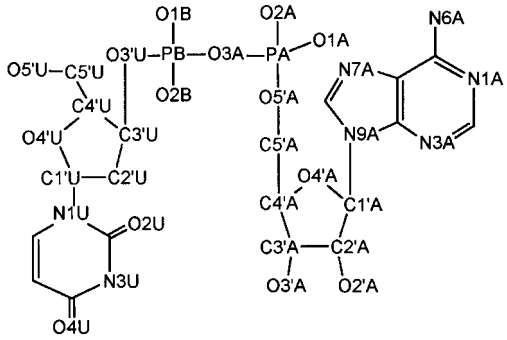

FIGURE 2: Numbering scheme for dUppA.

Table 5: Potential Hydrogen Bonds of RNase A with dUppA and pdUppA-3′-p[a]

RNase atom	inhibitor atom[b]	dUppA	pdUppA-3′-p[c]
Gln11 NE2	O2B	2.8	2.9
His12 NE2	O2B	2.8	2.4
Lys41 NZ	O3′U	(3.3)	3.1
Thr45 N	O2U	2.8	2.8
Thr45 OG1	N3U	2.9	2.8
Asn67 ND2	N1A	3.1	(3.4)
Gln69 OE1	N6A	(3.4)	3.1
Asn71 OD1	N6A	2.9	3.1
Asn71 ND2	N7A	2.9	3.2
His119 ND1	O2A	3.0	(3.4)
	O1B	3.1	2.8
Phe120 N	O1B	3.2	2.9

[a] Numbers in columns are distances in angstroms in the crystal structures of RNase A complexes with dUppA and pdUppA-3′-p (*26*). Interactions are listed if the distance between a donor (D) and an acceptor (A) is shorter than 3.3 Å and the angle D−H−A is greater than 90° in at least one of the complexes. Distances shown in parentheses are beyond the stated cutoff. [b] For nomenclature, see Figure 2. [c] Only potential hydrogen bonds involving the dUppA portion of pdUppA-3′-p are listed.

The interactions of dUppA (Figure 2) with RNase A are very similar to those made by the corresponding part of pdUppA-3′-p (Table 5; Figure 3A). The potential hydrogen bonds observed include two between uracil and Thr45; five connecting the 3′-α-phosphate with the side chains of Gln11, His12, Lys41, and His119 and the main chain of Phe120 at the catalytic site; and several between adenine and Asn71, Gln69, and Asn67. The 5′-α-phosphate of adenosine forms a hydrogen bond with ND1 of His119 that is not present in the pdUppA-3′-p complex and might make a functionally significant Coulombic interaction with NZ of Lys7, which is 4.4 Å away.

Modeling of the UppA·RNase A Complex. An initial model for the complex of RNase A with the substrate UppA was generated from the dUppA·RNase A crystal structure by

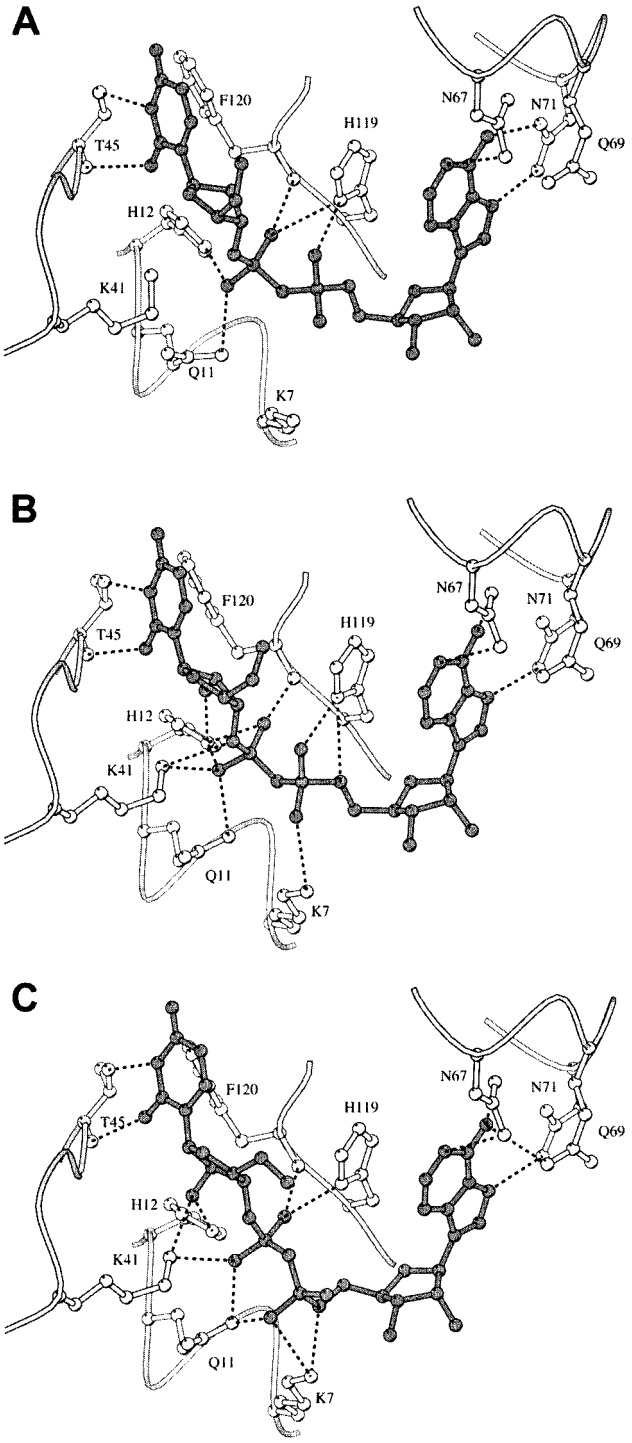

FIGURE 3: Potential interactions of RNase A with dUppA in the crystal structure of the complex (panel A) and with UppA in modeled complexes where the uridine ribose has C2′-endo (panel B) and C3′-endo (panel C) conformations. RNase residues are drawn with open bonds and atoms, and nucleotides have filled bonds and atoms. Hydrogen bonds are indicated by dashed lines. Diagrams drawn with MOLSCRIPT (*73*).

replacing a uridine 2′-H with an OH group. This model appeared to be defective in that the distance between the 2′-O and His12 was too large (3.6 Å) to allow the His NE2 group to catalyze deprotonation of the 2′-OH, as is expected in the initial step for substrate cleavage (see Discussion). Rotations of the His12 imidazole shortened this distance sufficiently but disrupted a hydrogen bond of His12 ND1 with the carbonyl O of Thr45 that helps to position the histidine. Alternative solutions were explored by examining other available crystal structures of RNase A complexes. The complex with UpcA (a UpA analogue in which a methylene group replaces the 5′-oxygen of the adenosine ribose; *51*, *52*) is the only one that involves a ribo substrate analogue, and in this structure, the distance between 2′-O and His12 NE2 (3.7 Å) is also beyond the required range. When the 2′-deoxyribose of thymidine was converted to ribose in the d(ApTpApApG) complex (PDB code 1rcn; *27*), the O−N distance (3.9 Å) was again too large. However, the analogous conversion in the d(CpA) complex (PDB code 1rpg; *28*) resulted in a much shorter O−N separation (2.7 Å). Therefore, a UppA model was made by (i) superimposing the d(CpA) and dUppA complex structures; (ii) removing RNase A from the d(CpA) complex, dA-5′-p from d(CpA), and dU from dUppA; (iii) transforming dC into U; (iv) altering torsion angles in the pyrophosphate to allow U to be connected with ppA; and (v) performing energy minimization of the complex. In this model (Figure 3B), the separation between uridine O2′ and His12 NE2 is 3.2 Å, i.e., within hydrogen-bonding range. The other intermolecular contacts are similar to those formed in the dUppA complex crystal structure: two potential hydrogen bonds from the crystal structure (N6A to Asn71 OD1; O1B to His119 ND1) are replaced by others (N6A to Asn67 OD1; O5′ to His119 ND1), while others are either maintained or optimized, and new contacts involving Lys7 (NZ to O1A) and Lys41 (NZ to O2B and O3′U) are formed.

In all of the crystal structures and models just described, the pyrimidine nucleoside ribose adopts a type S conformation (C2′-endo or C2′-endo/C3′-exo), so that C2′ is pushed away from His12. However, NMR studies have shown that in solution 58% of ribouridine molecules have a type N pucker (C3′-endo or C3′-endo/C2′-exo) rather than type S (vs 40% of 2′-deoxyuridines; *53*). Therefore, we also constructed a model UppA complex in which the uridine ribose is C3′-endo; the N pucker would place C2′ in closer proximity to His12, although the associated reorientation of C3′ would necessarily alter the positions of other groups on the dinucleotide. A model for free UppA with the desired ribose conformation was generated by connecting uracil and ppA from dUppA through a C3′-endo ribose taken from the crystal structure of the ppA-2′-p·RNase A complex (PDB code 1afl; *43*). This was subjected to energy minimization and docked to RNase A (from the dUppA complex structure) with AutoDock. The final model complex (Figure 3C) was then obtained by performing energy minimization. In this structure, uridine and the 5′-phosphate are displaced by ∼1−1.3 Å with respect to the corresponding groups in the dUppA complex, whereas the other parts of the dinucleotide superimpose much more closely. The shift of the uracil ring is not sufficient to disrupt the hydrogen bonds with Thr45, but these are perhaps not as well-optimized. NE2 of His12 is slightly less than 3.3 Å from O2′, within the estimated cutoff to allow deprotonation, and Lys41 NZ is now also positioned to interact with O2′. The potential hydrogen bond of His12 with O2B seen in the dUppA complex has been lost, but other interactions with the 3′-phosphate (involving Gln11, His119, and Phe120) appear to be maintained. The movement of the 5′-phosphate takes it away from His119 and places it within hydrogen-bonding distance of Lys7 and Gln11. Adenine forms the same interactions as in the dUppA

complex, but the 6-amino group is also now within hydrogen-bonding range of Asn67 OD1 and Gln69 OE1.

Cleavage of CppA by Angiogenin. The k_{cat}/K_m value for Ang with its best standard dinucleotide substrate, CpA, is 10^6-fold smaller than that measured with RNase A (*5*, *54*), in part reflecting weaker binding (*41*). The high K_m value for CpA (62 mM) precludes the use of this substrate for many types of structure−function and mechanistic studies; moreover, no other Ang substrates have proved suitable for these purposes thus far. In view of the large decrease in K_m for RNase A associated with the pyrophosphate internucleotide linkage, we considered it possible that CppA might be a "low-K_m" substrate for Ang that could be used in such experiments. HPLC-based assays with 94 μM CppA showed that this dinucleotide is indeed a substrate for Ang; the cleavage reaction followed first-order kinetics, and a value for k_{cat}/K_m of 1.27 ± 0.06 M^{-1} s^{-1} was obtained. This value is ~7-fold lower than that measured for CpA (8.4 ± 0.2 M^{-1} s^{-1}), a difference somewhat larger than that seen with RNase A (Table 2). The K_m for CppA was assessed by performing additional assays at a much higher substrate concentration. The value for v_0/[E] (where [E] is enzyme concentration) at 2.6 mM CppA was found to be 4.8×10^{-3} s^{-1}, as compared to 1.8×10^{-4} s^{-1} at 94 μM. Thus, the increase in v_0/[E] is nearly identical to that in substrate concentration, indicating that K_m must be well above 2.6 mM and most likely >10 mM. Inhibition assays with dUppA yielded a K_i value of 8.4 ± 0.1 mM.

DISCUSSION

Pyrophosphate-Linked Dinucleotides as Substrates for RNase A. Pancreatic RNase A and related enzymes are generally considered to have evolved primarily to catalyze the cleavage of P−$O^{5'}$ bonds after pyrimidine nucleotides in RNA via transphosphorylation (*55*, *56*). For RNase A, this reaction is extremely robust when the 5′ oxygen is provided by the preferred nucleoside adenosine, with k_{cat}/K_m values (>10^9 M^{-1} s^{-1}; *57*) approaching the highest measured for any enzyme. Catalysis of the subsequent hydrolysis that converts the cyclic 2′,3′-phosphate product to a 3′-phosphate proceeds at a ~1000-fold slower rate. RNase A has also been shown to cleave a variety of unnatural substrates in which a pyrimidine 3′ nucleotide is in phosphodiester linkage with a nonnucleotide. The simplest of these compounds, cytidine 3′-methyl phosphate and cytidine 3′-benzyl phosphate, have kinetic parameters similar to those of C>p (*29*). Uridine 3′-(5-bromo-4-chlorindol-3-yl) phosphate is cleaved at a comparable rate, although K_m is severalfold higher (*31*). Uridine 3′-(*p*-nitrophenyl) phosphate ($UpOC_6H_4$-*p*-NO_2) is a somewhat better substrate (*30*, *35*) but still 40−70× less efficient than UpA, mostly due to a difference in k_{cat} (*35*).

The present study identifies a new family of RNase substrates, the 3′,5′-pyrophosphate-linked dinucleotides, that are cleaved by RNase A almost as efficiently as standard dinucleotides. The k_{cat}/K_m values for CppA and UppA are only 4-fold lower than those of CpA and UpA, respectively, and are higher than for any other normal dinucleotides. The greater effectiveness of these nucleotides, as compared to the aforementioned non-RNA substrates, largely reflects their higher affinity for the enzyme. Indeed, the K_m for UppA is 70-fold lower than for UpA and 2-fold lower than for the tetranucleotide $dArU(dA)_2$, which is able to form interactions with additional base- and phosphate-binding sites (*58*). The structural basis for the higher affinity of the pyrophosphate linkage is apparent from the crystal structure of the complex of RNase A with dUppA. The 2′-deoxyuridine 3′-phosphate moiety binds in a manner nearly identical to the corresponding portions of d(CpA) (*28*) and d(ApTpApA) (*27*): the pyrimidine hydrogen bonds with Thr45, and the phosphate interacts with His12, His119, Gln11, and Phe120. Because of the increased size of the internucleotide linker, the adenine can be accommodated in its normal binding site only if the nucleoside conformation is syn, in contrast with the anti orientation for monophosphate-linked oligonucleotides. Remarkably, binding in this syn conformation, which places the 6-amino group in essentially the same position as for the anti adenosine in standard oligonucleotides, allows the formation of a similar number of hydrogen bonds. It is also possible that the stacking of the adenine with the His119 imidazole, which now involves the six- rather than the five-membered ring, is more favorable energetically. The "extra" moiety of UppA, the uridine 3′-β-phosphate, also appears to form productive contacts with the enzyme: in the dUppA complex, it lies within hydrogen-bonding distance of His119 and is positioned to form a medium-range Coulombic interaction with Lys7.

Is the effectiveness of dinucleoside pyrophosphates as RNase substrates merely fortuitous, or does it have biological relevance? Indeed, might pancreatic and related RNases have evolved to catalyze cleavage of such compounds as well as RNA? The results of studies with RNA 3′-terminal phosphate cyclases strongly suggest that 3′,5′-pyrophosphate internucleotide linkages exist in nature. These enzymes, which are expressed in all mammalian tissues and cells investigated (*59*), catalyze the addition of A-5′-p to the 3′-terminal phosphate of RNA in vitro, thereby generating a terminal NppA 3′,5′-pyrophosphate-linked dinucleotide (*32*). This is then cleaved to give the N>p and A-5′-p; cyclic 2′,3′-phosphates are found in many RNA species and are often required for RNA ligation (see ref *60*). NppA has been regarded as a chemically labile "activated" structure (due to the low pK_a of the 5′-phosphate leaving group) whose cleavage is nonenzymatic (*32*, *33*). However, we have shown here that 3′,5′-pyrophosphate ribonucleotide linkages are relatively stable: the half-life of UppA is >15 days at pH 6, 25 °C, and is likely to be no more than severalfold shorter at intracellular pH values and temperatures. Therefore, cleavage requires the action of an enzyme. Cyclization occurs rapidly with both purine and pyrimidine nucleoside 3′-phosphates. In the former case at least, it is clear that pancreatic RNase family enzymes, which are all pyrimidine specific, are not involved. However, these proteins might participate in the reaction with pyrimidine nucleotides. Moreover, it is possible that there are additional enzymatic pathways for generation of pyrimidine N>p moieties that also proceed via intermediate NppN′ structures and utilize such RNases.

Pyrophosphate-Linked Dinucleotides as Substrates for Angiogenin. Efforts to determine the effects of amino acid replacements or changes in reaction conditions on individual kinetic parameters for Ang-catalyzed reactions have been impeded by the lack of substrates with sufficiently low K_m

values. We investigated the possibility that the 3′,5′-pyrophosphate-linked dinucleotide substrates here developed for RNase A might fill this need. If NppA substrates bind to Ang 30−70-fold more tightly than the corresponding NpA substrates, as they do to RNase A, then the K_m value for CppA would be ∼1−2 mM, which is within the range that can be used for such experiments. Previous findings suggested that this might be the case: (i) dUppA-2′-p inhibits Ang with a K_i value of 150 μM (*24*); (ii) ppA binds only ∼10-fold less tightly than ppA-2′-p (*25*); and (iii) k_{cat}/K_m values for Ang-catalyzed cleavage of CpN substrates are at least 10-fold greater than for the corresponding UpN substrates (*25*). Nonetheless, the reduction in K_m imparted by the pyrophosphate linkage appears to be less than 6-fold. Our estimated lower limit for the K_m of CppA with Ang is 10 mM, making it unlikely that this substrate will be useful for analysis of changes in K_m and k_{cat} individually. However, addition of a 2′-phosphate might increase binding affinity sufficiently: dUppA-2′-p binds to Ang 56-fold more tightly than does dUppA.

Uncatalyzed Rate of UppA Cleavage. Nonenzymatic cleavage of ribonucleotide phosphodiesters has been investigated extensively at high pH values and/or high temperatures (reviewed in ref *61*). These studies have shown that the uncatalyzed reaction, like that catalyzed by RNase A, proceeds via a two-step transphosphorylation/hydrolysis mechanism. The initial product again is a cyclic 2′,3′-phosphate, but this is hydrolyzed to form a mixture of 2′- and 3′-phosphates rather than just the 3′-phosphate. Measurements under conditions that are more optimal for RNase assays (e.g., pH 6 at 25 °C) are problematic owing to the pervasive presence of RNases as laboratory contaminants. Thompson et al. (*62*) investigated the uncatalyzed rate of UpA cleavage at 25 °C in Mes buffer, pH 6, and measured a rate constant of 5×10^{-9} s^{-1}. However, the only uridine product detected was U>p. Because this is the same product formed by the RNase A-catalyzed reaction (RNase A hydrolyzes U>p considerably more slowly than it cleaves UpA), it is possible that the degradation observed was to some extent due to trace amounts of RNase A. Uncatalyzed dinucleotide cleavage at elevated pH values or temperatures yields predominantly the 3′- and 2′-phosphates with little accumulation of the cyclic nucleotide (*61*, *63*) (i.e., hydrolysis of the cyclic nucleotide appears to be much more rapid than dinucleotide transphosphorylation). It is unclear whether this is also the case at pH 6 and 25 °C. At this time, the value measured for UpA should be considered only an upper limit for the rate constant for the uncatalyzed reaction (k_{uncat}).

Our initial attempts to measure k_{uncat} for UppA were conducted at pH 6 (25 °C) and showed loss of the dinucleotide with concomitant production of only A-5′-p and U>p. Again, the correspondence between the observed products and those generated by RNase A raises the possibility that cleavage is not, in fact, uncatalyzed. Therefore, additional incubations were performed at pH 10, where the impact of any RNase A contamination would be expected to be less significant. U>p was still the only uridine product formed, demonstrating that uncatalyzed hydrolysis is much slower than transphosphorylation. If this is also the case at pH 6, then the rate of UppA cleavage measured at this pH (5.3×10^{-7} s^{-1}) might be the actual value for k_{uncat}. However, in the absence of any direct evidence for this, the measured rate constant can again be considered only as an upper limit. Cleavage of UpA at pH 10 proceeded 2500-fold more slowly than for UppA. If the same factor were to apply at pH 6, then k_{uncat} with UpA would be $< 2.1 \times 10^{-10}$ s^{-1} (i.e., $t_{1/2} >$ 150 years). The k_{uncat} values for UpA and UppA estimated here would translate into lower limits for the rate enhancements for RNase A-catalyzed cleavage (i.e., k_{cat}/k_{uncat}) of 1.3×10^{13} and 1.5×10^{7}, respectively.

Mechanistic Implications. A minimal mechanism for the RNase A-catalyzed transphosphorylation reaction was proposed 40 years ago (*64*, *65*) and is still consistent with all available structural and functional data (see ref *2*). In this mechanism, the imidazole ring of His12 acts as a base that deprotonates the 2′-hydroxyl of the substrate, facilitating its attack on the phosphorus atom. The pentacovalent species thereby generated breaks down to yield a cyclic 2′,3′-phosphate, aided by the acidic imidazolium ion of His119, which protonates the 5′ oxygen of the leaving group. The chemical nature of the pentacovalent species (transition state vs metastable phosphorane intermediate) has been the subject of debate, as has the precise role of His119 (*66*−*69*).

Replacements of His12 and His119 by Ala diminish k_{cat}/K_m values for cleavage of UpA and poly(C) by several orders of magnitude (*35*), in agreement with the standard mechanism. The substitution of His12 causes a comparable loss in activity toward $UpOC_6H_4$-*p*-NO_2 (*35*), indicating that the role of this residue in $UpOC_6H_4$-*p*-NO_2 cleavage is probably the same as with the traditional substrates, as would be expected if the imidazole deprotonates O2′. In contrast, replacement of His119 has essentially no effect when $UpOC_6H_4$-*p*-NO_2 is the substrate. This is again consistent with the proposed mechanism: the pK_a of the *p*-nitrophenolate leaving group is 7.14 [vs ≈14.8 for the nucleoside leaving groups in UpA and poly(C)] (*35*), and it is reasonable that participation of an acid is not required.

We find that with the substrate UppA, replacement of His12 by Ala lowers catalytic efficiency by 5−6 orders of magnitude, which is similar to the effect on UpA cleavage (Table 4). Thus, His12 appears to play largely the same role with both substrates. The decrease in k_{cat}/K_m for UppA produced by substitution of His119 is less substantial, 2000-fold, and is 54-fold smaller than the impact on the UpA reaction. This indicates that the His119 imidazole contributes less to UppA cleavage than to that of UpA but also that it fulfills some function in the UppA reaction that it does not play when $UpOC_6H_4$-*p*-NO_2 is the substrate. It is unlikely that this role is to protonate the 5′-O leaving group: the pK_a of the A-5′-p phosphate (∼6.4; *70*) is even lower than that of *p*-nitrophenol. However, the crystal structure of the complex of RNase A with dUppA reveals three potential interactions between His119 and the inhibitor (Table 5, Figure 3A): one hydrogen bond with a nonbridging oxygen on each phosphate and stacking with the six-membered ring of adenine.

We used modeling to investigate the likelihood that similar contacts are formed with the substrate UppA. Two models were generated, one with the uridine ribose in a C2′-endo conformation and the other with this ribose in a C3′-endo conformation. In both models (Figure 3B,C), His12 and O2′ are suitably juxtaposed for catalysis, and the other interactions are largely the same as those in the dUppA·RNase A crystal structure, with His119 again stacking against

adenine. However, in the C2′-endo model, His119 is positioned to hydrogen bond only to the 3′-β-phosphate of uridine (O2A and O5′) rather than to both phosphates, and in the C3′-endo model, it lies within hydrogen-bonding distance of the 3′-α-phosphate rather than the β-phosphate of uridine. Although we have not attempted to predict structures for the pentacovalent transition states that would be associated with these two ground-state models, it seems likely that such species would still form $\pi-\pi$ interactions and a hydrogen bond with His119. These interactions might be sufficiently energetic to account for the effect of His119 replacement on k_{cat}/K_m for UppA cleavage. Nevertheless, we cannot rule out the possibility that this activity decrease reflects the loss of a catalytic role for His119 in protonating a nonbridging phosphate oxygen of a phosphorane intermediate; in both ground-state models, the imidazole is positioned close to one of these oxygens.

What relevance do the present results on 3′,5′-pyrophosphate-linked dinucleotides have for the role of His119 in cleavage of normal substrates such as UpA? If the catalytic mechanisms with NpA and NppA are the same except that the NppA leaving group protonation is unassisted, this would imply that His119 accelerates the NpA reaction ∼50-fold by protonating the leaving group (the difference in the effects of His119 replacement with NpA and NppA) and ∼2000-fold (the effect of the replacement on NppA cleavage) through other means. Clearly, there are some major similarities in the mechanism by which RNase A catalyzes cleavage of the two classes of substrate: (i) the preferences for C vs U are identical, suggesting that pyrimidines form the same interactions in the transition state complexes; (ii) the catalytic efficiencies differ by only a factor of 4; and (iii) the replacement of His12 has comparable effects on cleavage of both types of substrates. However, there are potentially important differences vis-à-vis His119. In crystal structures of RNase A complexes with standard substrate analogues (*27*, *28*), the His imidazole stacks against the five-membered ring of adenine, but with dUppA, stacking involves the six-membered ring. In the complexes with monophosphate-linked inhibitors, His119 hydrogen bonds with an uncharged oxygen (O5′A), whereas in the dUppA complex and the UppA models it is positioned to hydrogen bond with either of two charged oxygens; the latter interactions are expected to be stronger (*71*). Thus, it seems likely that His119 contributes more to binding of NppA than NpA substrates.

ACKNOWLEDGMENT

We thank Dr. L. I. Irons for RNase A crystals, Dr. G. L. Gilliland for the RNase A·UpcA complex coordinates, and Dr. J. F. Riordan for helpful discussions.

REFERENCES

1. D'Alessio, G., and Riordan, J. F., Eds. (1997) *Ribonucleases*: *Structures and Functions*, Academic Press, New York.
2. Raines, R. T. (1998) *Chem. Rev. 98*, 1045−1065.
3. Richards, F. M., and Wyckoff, H. W. (1971) *Enzymes* (*3rd Ed.*) *4*, 647−806.
4. Eftink, M. E., and Biltonen, R. L. (1987) in *Hydrolytic Enzymes* (Neuberger, A., and Brocklehurst, K., Eds.) pp 333−375, Elsevier, New York.
5. Shapiro, R., Riordan, J. F., and Vallee, B. L. (1986) *Biochemistry 25*, 3527−3532.
6. Fett, J. W., Strydom, D. J., Lobb, R. R., Alderman, E. M., Bethune, J. L., Riordan, J. F., and Vallee, B. L. (1985) *Biochemistry 24*, 5480−5486.
7. Olson, K. A., Fett, J. W., French, T. C., Key, M. E., and Vallee, B. L. (1995) *Proc. Natl. Acad. Sci. U.S.A. 92*, 442−446.
8. Olson, K. A., and Fett, J. W. (1996) *Proc. Am. Assoc. Cancer Res. 37*, 57.
9. Iwama, M., Kunihiro, M., Ohgi, K., and Irie, M. (1981) *J. Biochem.* (*Tokyo*) *89*, 1005−1016.
10. Gullberg, U., Widegren, B., Arnason, U., Egesten, A., and Olsson, I. (1986) *Biochem. Biophys. Res. Commun. 139*, 1239−1242.
11. Domachowske, J. B., Dyer, K. D., Adams, A. G., Leto, T. L., and Rosenberg, H. F. (1998) *Nucleic Acids Res. 26*, 3358−3363.
12. Domachowske, J. B., Dyer, K. D., Bonville, C. A., and Rosenberg, H. F. (1998) *J. Infect. Dis. 177*, 1458−1464.
13. Ackerman, S. J., Gleich, G. J., Loegering, D. A., Richardson, B. A., and Butterworth, A. E. (1985) *Am. J. Trop. Med. Hyg. 34*, 735−745.
14. Lehrer, R. I., Szklarek, D., Barton, A., Ganz, T., Hamann, K. J., and Gleich, G. J. (1989) *J. Immunol. 142*, 4428−4434.
15. Durack, D. T., Ackerman, S. J., Loegering, D. A., and Gleich, G. J. (1981) *Proc. Natl. Acad. Sci. U.S.A. 78*, 5165−5169.
16. Fredens, K., Dahl, R., and Venge, P. (1982) *J. Allergy Clin. Immunol. 70*, 361−366.
17. Gleich, G. J., Loegering, D. A., Bell, M. P., Checkel, J. L., Ackerman, S. J., and McKean, D. J. (1986) *Proc. Natl. Acad. Sci. U.S.A. 83*, 3146−3150.
18. D'Alessio, G., Di Donato, A., Mazzarella, L., and Piccoli, R. (1997) in *Ribonucleases*: *Structures and Functions* (D'Alessio, G., and Riordan, J. F., Eds.) pp 383−423, Academic Press, New York.
19. Hofsteenge, J., Vicentini, A., and Zelenko, O. (1998) *Cell. Mol. Life Sci. 54*, 804−810.
20. Shapiro, R., and Vallee, B. L. (1989) *Biochemistry 28*, 7401−7408.
21. Shapiro, R., Fox, E. A., and Riordan, J. F. (1989) *Biochemistry 28*, 1726−1732.
22. Sorrentino, S., Glitz, D. G., Hamann, K. J., Loegering, D. A., Checkel, J. L., and Gleich, G. J. (1992) *J. Biol. Chem. 267*, 14859−14865.
23. Russo, N., and Shapiro, R. (1999) *J. Biol. Chem. 274*, 14902−14908.
24. Russo, A., Acharya, K. R., and Shapiro, R. (2001) *Methods Enzymol.*, in press.
25. Russo, N., Acharya, K. R., Vallee, B. L., and Shapiro, R. (1996) *Proc. Natl. Acad. Sci. U.S.A. 93*, 804−808.
26. Leonidas, D. D., Shapiro, R., Irons, L. I., Russo, N., and Acharya, K. R. (1999) *Biochemistry 38*, 10287−10297.
27. Fontecilla-Camps, J. C., de Llorens, R., le Du, M. H., and Cuchillo, C. M. (1994) *J. Biol. Chem. 269*, 21526−21531.
28. Zegers, I., Maes, D., Dao-Thi, M. H., Poortmans, F., Palmer, R., and Wyns, L. (1994) *Protein Sci. 3*, 2322−2339.
29. Witzel, H., and Barnard, E. A. (1962) *Biochem. Biophys. Res. Commun. 7*, 295−299.
30. Davis, A. M., Regan, A. C., and Williams, A. (1988) *Biochemistry 27*, 9042−9047.
31. Witmer, M. R., Falcomer, C. M., Weiner, M. P., Kay, M. S., Begley, T. P., Ganem, B., and Scheraga, H. A. (1991) *Nucleic Acids Res. 19*, 1−4.
32. Filipowicz, W., Strugala, K., Konarska, M., and Shatkin, A. J. (1985) *Proc. Natl. Acad. Sci. U.S.A. 82*, 1316−1320.
33. Hinton, D. M., Brennan, C. A., and Gumport, R. I. (1982) *Nucleic Acids Res. 10*, 1877−1894.
34. Shapiro, R., and Vallee, B. L. (1992) *Biochemistry 31*, 12477−12485.
35. Thompson, J. E., and Raines, R. T. (1994) *J. Am. Chem. Soc. 116*, 5467−5468.
36. delCardayré, S. B., Ribó, M., Yokel, E. M., Quirk, D. J., Rutter, W. J., and Raines, R. T. (1995) *Protein Eng. 8*, 261−273.
37. Moffat, J. G., and Khorana, H. G. (1961) *J. Am. Chem. Soc. 83*, 663−675.

38. Beaven, G. H., Holiday, E. R., and Johnson, E. A. (1955) in *The Nucleic Acids* (Chargaff, E., and Davidson, J. N., Eds.) pp 493−553, Academic Press, New York.
39. Shapiro, R., Fett, J. W., Strydom, D. J., and Vallee, B. L. (1986) *Biochemistry 25*, 7255−7264.
40. Shapiro, R., and Vallee, B. L. (1991) *Biochemistry 30*, 2246−2255.
41. Russo, N., Shapiro, R., Acharya, K. R., Riordan, J. F., and Vallee, B. L. (1994) *Proc. Natl. Acad. Sci. U.S.A. 91*, 2920−2924.
42. Harper, J. W., Auld, D. S., Riordan, J. F., and Vallee, B. L. (1988) *Biochemistry 27*, 219−226.
43. Leonidas, D. D., Shapiro, R., Irons, L. I., Russo, N., and Acharya, K. R. (1997) *Biochemistry 36*, 5578−5588.
44. Kabsch, W. (1993) *J. Appl. Crystallogr. 26*, 795−800.
45. Brunger, A. T., Krukowski, J., and Erickson, J. (1990) *Acta Crystallogr., Sect. A 46*, 585−593.
46. Morris, G. M., Goodsell, D. S., Halliday, R. S., Huey, R., Hart, W. E., Belew, R. K., and Olson, A. J. (1998) *J. Comput. Chem. 19*, 1639−1662.
47. Russo, N., Shapiro, R., and Vallee, B. L. (1997) *Biochem. Biophys. Res. Commun. 231*, 671−674.
48. Ukita, T., Waku, K., Irie, M., and Hoshino, O. (1961) *J. Biochem.* (*Tokyo*) *50*, 405−415.
49. Park, C., Schultz, L. W., and Raines, R. T. (2001) *Biochemistry 40*, 4949−4956.
50. Altona, C., and Sundaralingam, M. (1972) *J. Am. Chem. Soc. 94*, 8205−8212.
51. Richards, F. M., and Wyckoff, H. W. (1973) in *The Atlas of Molecular Structures in Biology* (Phillips, D. C., and Richards, F. M., Eds.) Clarendon Press, Oxford.
52. Gilliland, G. L., Dill, J., Pechik, I., Svensson, L. A., and Sjolin, L. (1994) *Protein Pept. Lett. 1*, 60−65.
53. Guschlbauer, W., and Jankowski, K. (1980) *Nucleic Acids Res. 8*, 1421−1433.
54. Shapiro, R., Harper, J. W., Fox, E. A., Jansen, H. W., Hein, F., and Uhlmann, E. (1988) *Anal. Biochem. 175*, 450−461.
55. Cuchillo, C. M., Pares, X., Guasch, A., Barman, T., Travers, F., and Nogues, M. V. (1993) *FEBS Lett. 333*, 207−210.
56. Thompson, J. E., Venegas, F. D., and Raines, R. T. (1994) *Biochemistry 33*, 7408−7414.
57. Park, C., and Raines, R. T. (2000) *FEBS Lett. 468*, 199−202.
58. Kelemen, B. R., Klink, T. A., Behlke, M. A., Eubanks, S. R., Leland, P. A., and Raines, R. T. (1999) *Nucleic Acids Res. 27*, 3696−3701.
59. Genschik, P., Billy, E., Swianiewicz, M., and Filipowicz, W. (1997) *EMBO J. 16*, 2955−2967.
60. Billy, E., Hess, D., Hofsteenge, J., and Filipowicz, W. (1999) *J. Biol. Chem. 274*, 34955−34960.
61. Oivanen, M., Kuusela, S., and Lönnberg, H. (1998) *Chem. Rev. 98*, 961−990.
62. Thompson, J. E., Kutateladze, T. G., Schuster, M. C., Venegas, F. D., Messmore, J. M., and Raines, R. T. (1995) *Bioorg. Chem. 23*, 471−481.
63. Jarvinen, P., Oivanen, M., and Lönnberg, H. (1991) *J. Org. Chem. 56*, 5396−5401.
64. Roberts, G. C., Dennis, E. A., Meadows, D. H., Cohen, J. S., and Jardetzky, O. (1969) *Proc. Natl. Acad. Sci. U.S.A. 62*, 1151−1158.
65. Findlay, D., Herries, D. G., Mathias, A. P., Rabin, B. R., and Ross, C. A. (1961) *Nature 190*, 781−784.
66. Breslow, R., and Chapman, W. H., Jr. (1996) *Proc. Natl. Acad. Sci. U.S.A. 93*, 10018−10021.
67. Anslyn, E., and Breslow, R. (1989) *J. Am. Chem. Soc. 111*, 4473−4482.
68. Gerlt, J. A., and Gassman, P. G. (1993) *Biochemistry 32*, 11943−11952.
69. Panov, K. I., Kolbanovskaya, E. Y., Okorokov, A. L., Panova, T. B., Terwisscha van Scheltinga, A. C., Karpeisky, M. Y., and Beintema, J. J. (1996) *FEBS Lett. 398*, 57−60.
70. Christensen, J. J., and Izatt, R. M. (1962) *J. Phys. Chem. 66*, 1030−1034.
71. Fersht, A. R., Shi, J. P., Knill-Jones, J., Lowe, D. M., Wilkinson, A. J., Blow, D. M., Brick, P., Carter, P., Waye, M. M., and Winter, G. (1985) *Nature 314*, 235−238.
72. Brünger, A. T. (1992) *Nature 355*, 472−475.
73. Kraulis, P. J. (1991) *J. Appl. Crystallogr. 24*, 946−950.

BI010888J